



# Reducing Lumbar Spine Vertebra Fracture Risk With an Adaptive Seat Track Load Limiter

Martin Östling<sup>1\*</sup>, Christer Lundgren<sup>2</sup>, Nils Lubbe<sup>1</sup> and Bengt Pipkorn<sup>1</sup>

<sup>1</sup>Autoliv Research, Vårgårda, Sweden, <sup>2</sup>System and CAE Department, Autoliv Sweden, Vårgårda, Sweden

## OPEN ACCESS

### Edited by:

Yong Han,  
Xiamen University of Technology,  
China

### Reviewed by:

Qing Zhou,  
Tsinghua University, China  
Fang Wang,  
Changsha University of Science and  
Technology, China

### \*Correspondence:

Martin Östling  
martin.ostling@autoliv.com

### Specialty section:

This article was submitted to  
Transport Safety,  
a section of the journal  
Frontiers in Future Transportation

Received: 05 March 2022

Accepted: 22 April 2022

Published: 08 June 2022

### Citation:

Östling M, Lundgren C, Lubbe N and  
Pipkorn B (2022) Reducing Lumbar  
Spine Vertebra Fracture Risk With an  
Adaptive Seat Track Load Limiter.  
Front. Future Transp. 3:890117.  
doi: 10.3389/ffutr.2022.890117

In future fully automated vehicles, sleeping or resting will be desirable during a drive. While a horizontal position currently appears infeasible, a relaxed seating position with a reclined seatback and an inclined seat pan which enables a safe, comfortable position for sleeping or resting is possible. However, the inclined seat pan increases the forces and moments acting on the lumbar spine of the occupant and thereby the risk of lumbar vertebra fractures in a frontal crash. An energy management system integrated into the longitudinal seat adjustment (a seat track load limiter: STLL) that can reduce this risk should be investigated. When evaluating the injury reduction potential of a new restraint system such as a STLL it is important to include variations in both occupant size and crash severity. Otherwise, there is a risk of sub-optimizing, that is, the restraint system is only working for a limited number of situations. The restraint systems addressing these variations are normally referred to as adaptive restraint systems. The first objective of the study is to develop an activation strategy (adaptive release time of the STLL) for different crash severities and occupant sizes, making full use of the available stroke distance without bottoming out the STLL. The second objective is to evaluate the potential of the adaptive STLL to reduce the risk of lumbar vertebra fractures by comparing it to 1) a fixed seat and 2) a passive version of the STLL. Simulated frontal impacts were performed with two male SAFER human body models (HBMs) as occupant surrogates: mid-sized (80 kg and 1.8 m) and large (130 kg and 1.9 m). Three crash pulse severity levels were evaluated: low (40 km/h), medium (50 km/h), and high (56 km/h) impact speeds. The fracture risk was evaluated for the five lumbar vertebrae (L1–L5) in three different seat conditions: 1) a seat fixed to the sled, 2) a passive STLL that moves when a given force is exceeded, and 3) an adaptive STLL which moves at a time that depends on the occupant mass and crash pulse severity. The risk for lumbar vertebra fracture increased with crash pulse severity, while HBM size had no effect on risk. For all conditions, the passive STLL reduced injury risks compared to the fixed seat, and the adaptive STLL reduced risk even further.

**Keywords:** adaptive restraint, automated vehicles, human body model, lumbar vertebra fracture, occupant restraint system, relaxed seating position, seat track load limiter

## 1 INTRODUCTION

With the introduction of automated vehicles, the driver task will no longer be required, making it possible for the driver to engage in other tasks. Resting and sleeping are highly rated in surveys as desirable activities during a car ride (Koppel et al., 2019), particularly for longer trips (Östling and Larsson, 2019). When sleeping, a supine (horizontal, seatback fully reclined) position is preferred (Stanglmeier et al., 2020; Caballero-Bruno et al., 2021). However, the limited cabin space in most passenger cars prevents fully supine positions. Furthermore, current seatbelts are designed to load the strong parts of the occupant's body, traveling across the pelvis, over the shoulder, and across the chest, allowing a controlled forward motion during the crash (Adomeit and Heger, 1975; Adomeit, 1977). Any occupant position that is not upright, e.g., reclined or supine, compromises loading and control of the pelvis and chest, with submarining (the pelvis sliding under the lap belt, causing the lap belt to intrude into the soft abdomen) as a likely consequence (Dissanaike et al., 2008; McMurry et al., 2018; Boyle et al., 2019).

A relaxed position, with a reclined seatback and an inclined seat pan, is comfortable for sleeping (Stanglmeier et al., 2020). A relaxed position increases seatback inclination compared to what is commonly referred to as reclined position and is more challenging for occupant protection (Östling et al., 2021). However, during a frontal crash, the inclined seat pan provides most of the restraining force and control of the forward movement of the lower body, thereby reducing the risk of submarining and the dependence on the lap and shoulder seatbelt (Wiechel and Bolte 2006). This added restraining force is especially important, as the relaxed position requires a seat away from the instrument panel and thereby makes it infeasible to restrain the lower body in the traditional way with a knee bolster or knee airbag as proposed in earlier studies (Ji et al., 2017; Rawska et al., 2019; Tang et al., 2020; Rawska et al., 2021). However, a reclined position induces compression forces to the lumbar vertebrae because they are in line with the impact direction (Boyle et al., 2019). This increases the fracture risk, particularly for the first lumbar vertebra, L1 (Richardson et al., 2020). In addition to the L1 fractures, Richardson et al. (2020) also reported rib, sternum, and pelvis wing fractures from 50 km/h frontal sled tests with post mortem human subjects (PMHS) in reclined seating position.

To address the increased forces and moments acting on the lumbar vertebrae in the relaxed position (reclined seatback and inclined seat pan), Sengottu-Velavan and Huf (2018) incorporated an energy management system in the longitudinal seat adjustment in a concept seat (the system, a seat track load limiter, is hereafter referred to as a passive "STLL"). That passive STLL (the seat moves when a given force is exceeded) substantially reduced the lumbar spine compression force and flexion moment for different anthropomorphic test devices (ATDs). Östling et al. (2021) further improved the concept by making the STLL actively controlled (the seat was initially fixed to the vehicle and then released by activation of a pyrotechnical unit at a fixed pre-defined time). The active STLL further reduced the lumbar spine

force in tests with a Test Device for Human Occupant Restraint 50th percentile male (THOR-50M). However, Östling et al. (2021) highlighted the need for an activation strategy that considers occupant's mass and crash severity, to avoid reaching the limit of the forward displacement of the seat track ("bottoming out"). The energy absorbing elements in the seat have also been shown to reduce the risk for whiplash injury in rear impacts (Luo and Zhou, 2010; Zhang and Zhou, 2016).

The effect of variation in the occupant's mass can be investigated with ATDs to some extent. They are available in three adult sizes, representing the heights and masses of a 5th percentile female, a 50th percentile male, and a 95th percentile male (Mertz et al., 1989). However, the sizes are based on US population measurements of height and mass from the 1970s (Schneider et al., 1983). More recent data have shown that the 50th and 95th male ATDs' masses corresponded to the 33rd and 81st percentiles, respectively, of the current US population (Reed and Rupp, 2013).

The intention of this investigation is to design robust restraint systems for a diverse population by covering 95% of the population in terms of occupant mass. Morphable FE HBMs can be designed to simulate the whole range of occupant anthropometry by parametric morphing (Hwang et al., 2016). The first objective of the study is to develop an activation strategy (adaptive release time of the STLL) for different crash severities and occupant sizes (enabled by parametric morphed HBMs), making full use of the available seat stroke distance without bottoming out the STLL. The second objective is to evaluate the potential of the adaptive STLL to reduce the risk of lumbar vertebra fractures by comparing it to 1) a fixed seat and 2) a passive version of the STLL.

## 2 MATERIALS AND METHODS

Finite element (LS-Dyna, R9.3.1 R140922, LSTC) frontal sled simulations were executed using three different crash pulse severities and two different anthropometries of the SAFER HBM v9 with a reclined seatback and inclined seat pan. The influence on lumbar vertebrae fracture risk was investigated for three seat track configurations: the seat fixed to the sled, a passive STLL, and an adaptive STLL. Unlike the passive STLL, which moves when a given force is exceeded, the adaptive STLL's release mechanism timing is dependent on an activation strategy that adapts to the occupant mass and the predicted crash severity.

### 2.1 Occupant Surrogates

The US National Health and Nutrition Examination Survey (NHANES) data from 2011–2014 (Fryar et al., 2016) was used to define a large 65-year-old occupant (95th percentile) who would challenge the STLL by reaching the limit of the forward displacement (bottoming out). Starting with the validated SAFER HBM v9 mid-sized male (80 kg and 1.8 m), parametric HBM morphing with statistical human shape target geometries from Hwang et al. (2016) generated an HBM matching the sex, age, stature, and mass of the large male anthropometry (130 kg and 1.9 m); see **Figure 1**.

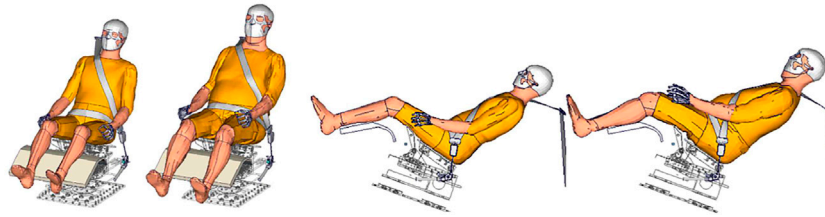


**FIGURE 1** | SAFER HBM v9 positioned on the generic seat with seatbelt routed. Left: front views of a mid-sized male and a large male. Right: side views of a mid-sized male and a large male.

**TABLE 1** | Cross-section area in mm<sup>2</sup> for L1–L5 for the two HBMs.

HBM	L1	L2	L3	L4	L5
Mid-sized male	1049	1142	1137	1140	1323
Large male	1366	1585	1558	1433	1450

The SAFER HBM v9 was originally developed from the Total Human Model for Safety (THUMS) v3 (Iwamoto et al., 2002), for the purpose of improving the understanding of impact response and injury mechanisms for car occupants. The SAFER HBM v9 has an updated rib cage (Iraeus and Pipkorn, 2019) and lumbar spine (Östh et al., 2020). Moreover, the SAFER HBM v9 has been validated to predict the kinematics and rib fracture risk of an upright seated occupant (Pipkorn et al., 2019) and the kinematics of a reclined seated occupant (Mroz et al., 2020). The parametric morphed versions of the SAFER HBM v9 include females and males of various anthropometries (including a large male), which were validated by means of PMHS tests in both frontal and lateral impact conditions (Larsson et al., 2021).

### 2.2 Risk of Lumbar Vertebrae Fracture

The risk of lumbar vertebra fractures was evaluated with the recently proposed injury risk function for combined compression flexion loading of the lumbar vertebra (Tushak et al., 2022) in the SAFER HBM v9. The injury risk function is based on censored force and moment failure data from three-vertebrae lumbar segments tested in combined compression flexion. 40 spine segments were tested. The injury risk function is based on a linear combination of stresses from the axial compression (force divided by cross-section area: CSA) and flexion moment (moment divided by CSA<sup>3/2</sup>) expressed as the predictor variable, L (Eq. 1). The function also includes a weighting factor to account for the relative contributions of force and moment to failure (Eq. 1). The age (in years) is included as a covariate (Eq. 2).

$$L(t) = (1 - 0.11) \frac{F(t)}{CSA} + 0.11 \frac{M(t)}{CSA^{3/2}}, \quad (1)$$

$$P(fracture|L, Age) = 1 - e^{-\left[\frac{L(t)}{e^{1.896 - 0.00874 \cdot Age}}\right]^{0.201}}. \quad (2)$$

In the HBM simulations, lumbar vertebra forces and moments were extracted in the L1–L5 vertebrae using cross-

section force-moment measurements. The cross-sections were defined for each vertebra, including the cortical and trabecular bones of the vertebral body as well as the transverse and spinous processes (Mroz et al., 2020; Mroz et al., 2022). The cross-section areas were calculated for L1–L5 for both the mid-sized male and the large male; Table 1. The forces and moments from all five vertebrae as well as each vertebra cross-section area are used in Eqs 1, 2 to assess the risk of injury for each vertebra for 45- and 65-year-old occupants as it has been reported that the risk of lumbar vertebra fracture is age-dependent (Jakobsson et al., 2006; Bilston et al., 2011; Rao et al., 2014).

The risk of two or more fractured ribs (AIS2+) was calculated and evaluated, in order to ascertain whether there were any negative effects from the STLL on other body areas. The rib fracture risk was calculated using a strain-based probabilistic method based on peak strains in the cortical bone of each rib (Forman et al., 2012) and the Weibull smoothed injury risk function for 45- and 65-year-old occupants (Iraeus, 2015).

### 2.3 Restraint System and STLL

The investigation was carried out for belted HBMs seated in a relaxed position (seatback reclined to 60° and seat pan inclined to 35°) in a generic semi-rigid seat with a rigid seatback, and lower leg support, as described by Östling et al. (2021). The HBMs were restrained by a seat-integrated three-point seatbelt system comprising two 2 kN lap belt pretensioners (buckle and end-bracket) to avoid submarining (Östling et al., 2017; Richardson et al., 2020). In addition, the seatbelt system included a shoulder belt retractor with a 2 kN pretensioner and 4 kN load limiter and a crash locking tongue, preventing webbing slippage from the shoulder belt to the lap belt (or vice versa). The activation times of the pretensioners were as in the work by Östling et al. (2021), with the buckle pretensioner activated at 2 ms and the shoulder belt and end bracket pretensioners activated at 9 ms. The STLL force levels were also provided by Östling et al. (2021), who tuned the force levels of the active (30 ms release time) and passive STLLs in order to achieve 0.2–0.25 m seat stroke distance in a 50 km/h crash pulse, using the THOR-50M in a generic seat weighing 130 kg. 0.25 m was chosen as the maximum stroke distance as this is approximately the adjustment range of drivers’ seats in passenger cars (Bohlin et al., 1978).

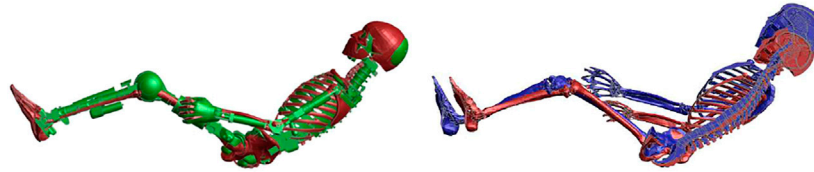


**FIGURE 2** | Left: overlay of SAFER HBM v9 mid-sized male (red) and THOR-50M (green). Right: overlay of SAFER HBM v9 mid-sized male (red) and morphed large male (blue).

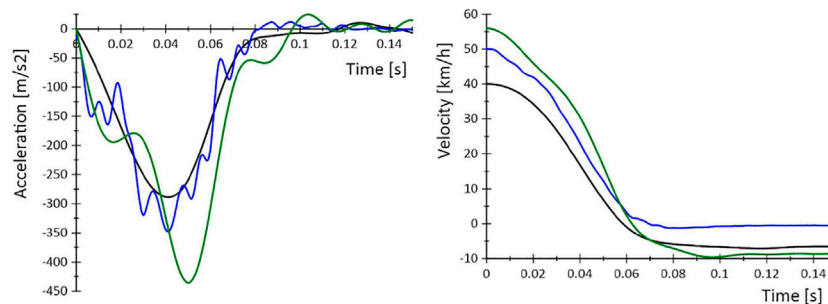


**FIGURE 3** | Left: acceleration vs. time. Right: velocity vs. time. For both figures, the black curves represent the low-severity crash pulse (40 km/h), the blue curves represent the mid-severity crash pulse (50 km/h), and the green curves represent the high-severity crash pulse (56 km/h).

## 2.4 HBM Positioning

Using an in-house positioning tool, the SAFER HBM v9 was positioned to match the test position of the THOR-50M described by Östling et al. (2021). First, the SAFER HBM's H-point was positioned at the corresponding H-point of the THOR-50M (20 mm rearward and 20 mm downward compared to the THOR H-point). Second, the SAFER HBM v9 pelvis was rotated around the H-point to match the angle of the THOR-50M. Finally, the thorax, neck, head, arms, and legs were rotated to match the position of the THOR-50M; see **Figure 2**. The large male HBM's H-point was positioned according to the H-point of the mid-sized male HBM. Then the pelvis was rotated around the H-point to match the pelvis shape, with a focus on the notch angle, the angle created by a line that connects the anterior superior iliac spine (ASIS) and the anterior inferior iliac spine (AIIS) measured to the horizontal axis (Moreau et al., 2021). Care was taken with the ASIS and AIIS area because it is an important support area for the lap belt and provides a good overall overlay of the pelvis. The thorax, neck, head, arms, and legs were adjusted to line up with the mid-size male; see **Figure 2**. The final positions of the HBMs, seated in the relaxed position on a generic seat with the belts routed, are shown in **Figure 1**.

## 2.5 Crash Pulses

Three full frontal crash pulses, varying in severity, were used in the analysis, see **Figure 3**. An HBM simulation of a 50 km/h crash pulse (mid-severity), also used by Östling et al. (2021), was compared to the results from the sled test result with THOR-50M. The high-severity crash pulse at 56 km/h (Dobberstein et al., 2021; Höschele et al., 2021) challenged the seat track

load limiter, potentially provoking bottoming out in combination with the HBM of a large male. A low-severity crash pulse at 40 km/h (Dobberstein et al., 2021; Höschele et al., 2021) represented a crash velocity at which the majority of occupants get injured (Forman and McMurry, 2018). Injury risk reduction at the low-severity crash pulse has a large effect on the overall number of injuries.

## 2.6 Simulations

In the first stage, the simulation model was validated by means of mechanical sled tests performed in the set-up used by Östling et al. (2021); see **Supplementary Appendix SA**. The mass of the generic seat used in the tests was 130 kg. The mass of a production seat with a seat-integrated seatbelt was replicated by reducing the seated mass to 70 kg (Östling et al., 2021). The force-displacement characterization used by Östling et al. (2021) (both the passive and the adaptive STLL force levels) was adjusted to reach the same stroke distance for the new seat mass. The adaptive STLL force-displacement characteristics started at 19.6 kN at 0.012 m and increased progressively to 31.6 kN at a forward displacement of 0.25 m, while the passive STLL started at 20.6 kN at 0.012 m and reached 35.1 kN at 0.25 m; see **Figure 4**.

In a second stage, the simulations of the adaptive STLL were performed starting with a 30 ms release time (used by Östling et al., 2021), for all HBM and crash pulse severity combinations. Depending on how the resulting seat stroke distance related to the maximum allowed distance (0.25 m), the release time was either decreased (as for the mid-sized male in the low-severity crash pulse), kept constant (for the mid-sized male in the mid-severity crash pulse), or increased (all other combinations). The decrease

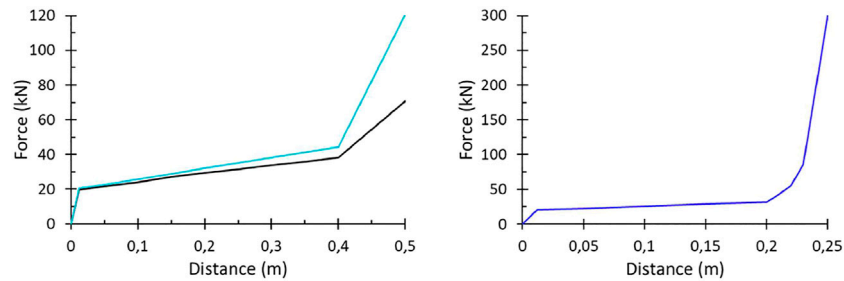


**FIGURE 4** | Left: STLL force characteristics vs. displacement for adaptive (black) and passive without soft stop (light blue). Right: STLL force characteristics vs. displacement for passive with a soft stop limit the seat stroke to 0.25 m (dark blue).

and increase in release time were performed in 10 ms steps until the maximum seat stroke distance was reached. However, as crash severity estimation, needed in order to calculate the adaptive release time, assumed to be done in-crash, similar to current crash severity estimation used to activate dual-stage airbags (Takata Corporation, 2017), release time less than 20 ms was not allowed. If the resulting seat stroke distance was less than 0.22 m, a 5 ms increase in release time was simulated to complement the final 10 ms step. These simulations were performed to demonstrate the need for an adaptive release and to provide suitable release times to be used for risk calculations. The results are presented in **Section 3.2**. The risks for lumbar vertebra fracture and rib fracture were only calculated for the seat track distances that best met the 0.25 m seat stroke requirement.

In a third stage, the simulations of the passive STLL were performed for all HBMs and crash pulse severity combinations using the force defined by Östling et al. (2021). As with the simulations with a 30 ms release time for the adaptive STLL, many of the simulations exceeded the 0.25 m seat stroke distance. A “soft stop” was therefore implemented at the passive STLL to limit the seat stroke to 0.25 m: starting at 0.2 m, the STLL force ramps up to 55 kN at 0.22 m, 86 kN at 0.23 m, and 300 kN at 0.25 m; see **Figure 4**. Additional simulations were then performed with the soft stop. These simulations were performed to demonstrate the need for a soft stop in addition to the force-displacement characteristics proposed by Östling et al., 2021. The results are presented in **Section 3.3**. Similar to the adaptive STLL, the risks for lumbar vertebra fracture and rib fracture were only calculated for seat track distances less than 0.25 m.

The three simulation steps: validation, adaptive STLL, and passive STLL are visualized in a flow chart in **Supplementary Appendix SB**.

## 3 RESULTS

### 3.1 HBM Kinematic Response

The crash kinematics followed the same overall pattern at the three crash severities for both HBMs. The seatbelt pretensioners held the HBM against the seat pan and seatback. The pelvis started to translate forward where it

compressed the seat pan springs and started to load the lap belt but the angled seat pan prevented the pelvis from translating forward notably. Submarining did not occur in any of the simulations. The longest pelvis displacement occurred for the high-severity crash pulse with the fixed seat: 163 and 234 mm in the  $x$ -direction for the mid-size male and large male, respectively. The torso was effectively restrained by the shoulder belt which prevented any larger forward displacement. The longest torso displacements, measured at the first thoracic vertebra (T1), were observed with the fixed seat and the high-severity crash pulse: 331 mm and 325 mm in the  $x$ -direction for the mid-size male and large male, respectively. The initial relaxed position of the upper body prevented upward forward rotation of the torso; however, the head rotated forward (under flexion moment) until it touched the chest. The legs and feet moved forward more than the pelvis when the knee joints straightened. The crash kinematics are exemplified in **Figure 5**, showing the mid-sized male in the fixed seat in 20 m increments after the high-severity crash pulse (at 0 m).

### 3.2 Release Times of the Adaptive STLL

Seat stroke distance and peak force in the adaptive STLL for all simulations are presented in **Table 2**. The simulations with 30 ms release times resulted in excessive seat stroke distances: 0.37, 0.30, 0.35, and 0.48 m (for the mid-sized male with the high-severity crash pulse and the large male with the low-, mid-, and high-severity crash pulses, respectively). On the other hand, the seat stroke distance was too short for the mid-sized male in the low-severity crash pulse (0.2 m). After adjusting the release times to fulfill the 0.25 m requirement, they were all in the interval of 20–60 ms. As the crash severity increased, the release times for both HBMs increased. The release times that best met the 0.25 m seat stroke requirement are highlighted by an underlined release time value in **Table 2**. The injury risk was calculated for these underlined cases only.

### 3.3 Passive STLL With and Without Soft Stop

For all simulations with the passive STLL, the seat strokes and peak forces (with and without the soft stop) are presented in **Table 3**. The simulations without the soft stop resulted in too

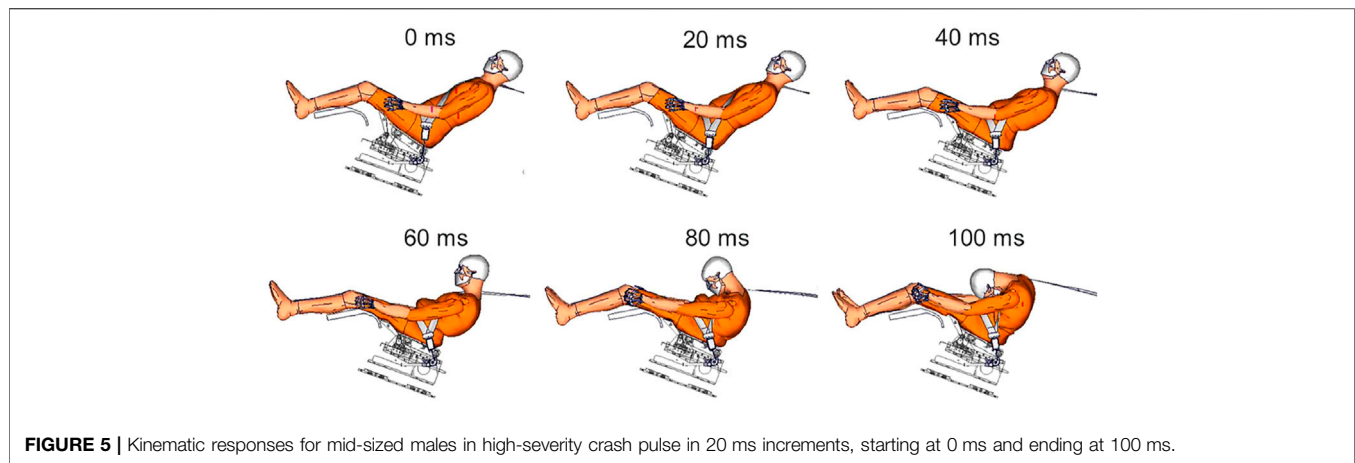


**FIGURE 5 |** Kinematic responses for mid-sized males in high-severity crash pulse in 20 ms increments, starting at 0 ms and ending at 100 ms.

**TABLE 2 |** Release time and corresponding seat stroke distance and peak force in the STLL for the adaptive STLL simulations.

Case	Crash pulse severity	HBM size	Release time (ms)	Seat stroke distance (m)	Peak force STLL (kN)
1	Low	Mid-sized male	30	0.20	29.4
2	Low	Mid-sized male	20	0.21	30.0
3	Low	Large male	30	0.30	33.7
4	Low	Large male	40	0.27	32.3
5	Low	Large male	45	0.24	31.1
6	Low	Large male	50	0.21	29.7
7	Mid	Mid-sized male	30	0.24	31.3
8	Mid	Large male	30	0.35	36.1
9	Mid	Large male	40	0.30	33.7
10	Mid	Large male	45	0.26	32.0
11	Mid	Large male	50	0.21	30.2
12	High	Mid-sized male	30	0.37	36.9
13	High	Mid-sized male	40	0.33	35.1
14	High	Mid-sized male	50	0.24	31.2
15	High	Large male	30	0.48	63.6
16	High	Large male	50	0.38	37.1
17	High	Large male	60	0.25	31.5

**TABLE 3 |** Seat stroke distance and peak force in the STLL for in the passive STLL simulations with and without soft stop.

Case	Crash pulse severity	HBM size	Soft stop	Seat stroke distance (mm)	Peak force STLL (kN)
1	Low	Mid-sized male	No	0.19	31.2
2	Low	Mid-sized male	Yes	0.19	31.1
3	Low	Large male	No	0.27	36.6
4	Low	Large male	Yes	0.23	84.5
5	Mid	Mid-sized male	No	0.23	34.1
6	Mid	Mid-sized male	Yes	0.22	56.1
7	Mid	Large male	No	0.33	40.0
8	Mid	Large male	Yes	0.24	169.7
9	High	Mid-sized male	No	0.34	40.8
10	High	Mid-sized male	Yes	0.24	196
11	High	Large male	No	0.44	76.7
12	High	Large male	Yes	0.25	275.6

long seat stroke distances: 0.34 m for the mid-sized male in the high-severity crash pulse, and 0.33 m, and 0.44 m for the large male in mid and high-severity crash pulse, respectively.

After implementing the soft stop starting at 0.22 m, all seat stroke distances met the 0.25 m requirement. The injury risk was only calculated for simulation with the soft stop.

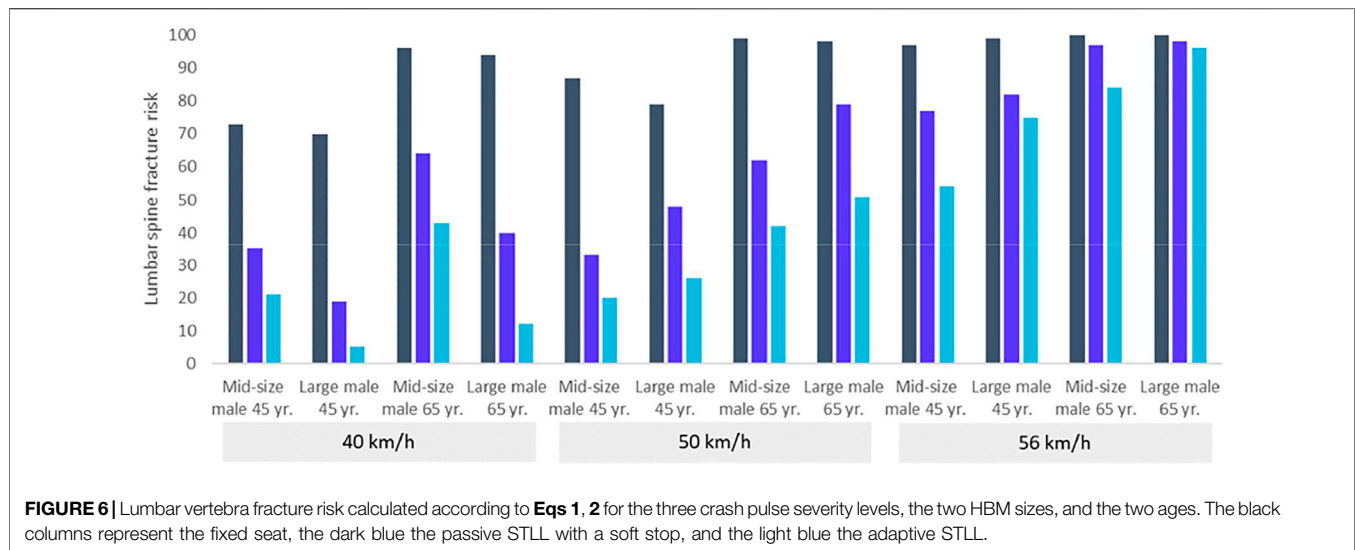


**FIGURE 6** | Lumbar vertebra fracture risk calculated according to Eqs 1, 2 for the three crash pulse severity levels, the two HBM sizes, and the two ages. The black columns represent the fixed seat, the dark blue the passive STLL with a soft stop, and the light blue the adaptive STLL.

### 3.4 Lumbar Vertebra Fracture Risk

The maximum lumbar vertebra fracture risks for the two HBMs in the three crash pulse severity levels (calculated according to Eqs 1, 2) are presented in Figure 6. For all the scenarios, the highest risk was seen for L1. The corresponding L1 compression forces and flexion moment are in Supplementary Appendix Figures SD1, SD2. The fracture risk was similar for the two HBMs and increased with age and crash pulse severity. While the passive STLL with a soft stop and the adaptive STLL both reduced the fracture risk for all scenarios, the adaptive STLL had the lowest risk. However, for the high-severity crash pulse, the risk of lumbar fractures is never below 50%.

The risk of two or more fractured ribs (AIS2+) was calculated using the injury risk curves for 45- and 65-year-old occupants (Iraeus, 2015) for both the mid-sized male and the large male in the three crash pulse severities; results are in Supplementary Appendix Tables SC1–SC3. The rib fracture risk increased with age and crash pulse severity; while risk was substantially reduced in simulations with both versions of the STLL, the adaptive STLL produced the lowest risk.

## 4 DISCUSSION

Each combination of HBM size and crash severity level required an individual release time to avoid bottoming out the STLL, while using the available stroke distance. Moreover, it was shown that the STLL with an adaptive release time achieved lower lumbar vertebra fracture and rib fracture risks than the passive STLL—for every combination.

The simulations with the SAFER HBM v9 of a mid-sized male in the relaxed position supported the test results with THOR-50M (Östling et al., 2021), both indicating a reduced risk of lumbar spine vertebra fracture using the STLL. A more severe crash pulse and/or the heavier HBM demonstrated the need for an adaptive release time to guarantee a seat stroke distance of less than 0.25 m. However, the SAFER HBM

showed a substantial reduction in risk for thorax injury (risk of rib fractures) with the mid-severity crash pulse (50 km/h) using the STLL. In contrast, the tests with THOR-50M indicated an increased risk of thorax injury, when measured as the maximum of the resultant value from the four infra-red telescoping rods for the assessment of chest compression (IR-TRACCs): Rmax or a slight decrease when measured as the maximum longitudinal value from the four IR-TRACCs: Xmax for the STLL (Östling et al., 2021). This difference supported the statement of Östling et al. (2021): “We believed HBMs with human-like design and use of rib strain as an indicator of risk of rib fracture, are likely to be more biofidelic than chest deflection to evaluate a potential increase or decrease in risk of rib fractures in reclined and relaxed positions”.

With the HBM in the relaxed position in the fixed seat, the lumbar vertebra fracture risk is already high with the low-severity crash pulse (73% and 96% for the 45-year and 65-year-old mid-sized males, respectively). Although the adaptive STLL reduces the risk substantially, by reducing both the components of the injury risk predictor, compression force, and flexion moment (see Supplementary Appendix Figures SD1, SD2), it fails to reduce the injury risk below 25% for the 65-year-old mid-sized male at any crash severity level. Furthermore, with the high-severity crash pulse, the risk is above 50% for all HBMs. To put this percentage in perspective, a 25% risk of sustaining an AIS3+ injury is often used as a threshold value for assessing acceptable crashworthiness using ATDs (Craig et al., 2020), and a major compression burst fracture of the lumbar vertebra is defined as an AIS3 injury (AAAM, 2015). The reason for the adaptive STLL’s inability to reduce the risk of injury in the high-severity crash pulse is the relatively late release time required to keep the seat stroke distance below 0.25 m (the release times were 50 ms for the large male with the 50 km/h crash pulse and the mid-sized male with the 56 km/h crash pulse, and 60 ms for the large male with the 56 km/h crash

pulse). At these times, the maximum forces in the lumbar vertebrae have just about been reached; see **Supplementary Appendix Figure SD1**. The STLL force levels were initially designed for the THOR-50M with a 50 km/h crash pulse (Östling et al., 2021). Designing the STLL force level for the large male with the high-severity crash pulse instead would enable an earlier release time and a concomitant lower risk of lumbar vertebra fracture. However, the consequence of a higher STLL force level is higher injury risks in the low- and mid-severity crash pulses. Clearly, any optimization targeting equal risks, i.e., the same probability of injury in various conditions, has its downsides. While most car crashes occur at a relatively low speed (20 km/h) with low injury risk, the majority of injuries occur at approximately 40 km/h (Forman and McMurry, 2018). As a result, risk reductions at 40 km/h are estimated to result in the largest absolute number of injuries prevented. With this statistic in mind, the force level used in this study is recommended. Another way to reduce the risk of sustaining injury in high-severity crash pulses without increasing it in low- and mid-severity crash pulses is to implement either longer seat stroke distances or dual force levels for the STLL. Both these ideas enable earlier release times for the high-severity crash pulse.

To enable individual release times (calculated with an activation strategy), classifications of the crash severity and occupant's mass are needed. To predict and classify crash severity, an in-crash algorithm similar to the one used to select single- or dual-stage activation of the driver airbag might be feasible, as the earliest time for activation is similar—around 20 m after first contact (Takata Corporation, 2017). To detect and classify the occupant mass, an onboarding occupant monitoring system is needed. This investigation included two different HBM sizes; however, a future monitoring system might have the capacity to detect finer mass differences between occupants with a concomitant ability to calculate new release times.

To improve the activation strategy further, information about the seat position (i.e., available stroke distance given any initial seat position) and potential activation of frontal airbags could be included. In addition, the crash pulses with a lateral component, like a frontal oblique crash, should also be analyzed to evaluate whether the STLL is negatively affected: the lateral force might prevent the seat from moving along the track. More research and development are needed to explore the full potential of the system.

The equations to calculate lumbar vertebrae fracture risk are based on the linear combination of stresses from the axial compression (force/cross-section area) and flexion moment (moment/cross-section area<sup>3/2</sup>) with a weighting factor of 0.11. This means that the calculated risk comes mainly from the compression force, which increases with body mass and crash pulse severity. However, because the force is divided by the vertebrae cross-section area, which is larger for the large male, the risk is actually higher for the mid-size male. (This difference is not seen in the high-severity crash pulse results, due to the late release time required to avoid bottoming out the STLL for the large male). An obese mid-

size male or female appears to be the most challenging anthropometry (e.g., relatively heavy body mass and relatively small vertebral cross-section).

Alternative risk functions addressing lumbar vertebra fractures have been proposed by Stemper et al. (2018) and Ortiz-Paparoni et al. (2021). The former's was based on compression forces at the lumbar spine measured in drop tower tests, from 23 PMHS lumbar specimens. The flexion moment was found to have some (albeit small) influence on the fracture risk, so it was included in the risk function proposed by Tushak et al. (2021). Ortiz-Paparoni et al. (2021) carried out a combined analysis from tests with 75 PMHS lumbar spines. Based on the test results, they developed an injury risk function using a combined metric. The intercept value for the flexion moment was higher than the moment at fracture that Tushak et al. (2021) obtained in lumbar spine testing and therefore the risk function proposed by Tushak et al. (2021) was considered more appropriate for the study.

Parameterized morphing of HBMs enabled us to use statistical data to generate HBM versions of different anthropometries. However, the individual variation of humans is large, and we have only evaluated one (average) version each of the mid-sized and the large males. Furthermore, as noted, the vertebral cross-section area has a large effect on the risk of lumbar vertebra fracture. A 10% increase or decrease for a 1000 mm<sup>2</sup> cross-section area with 4500 N lumbar vertebrae compression force and 100 Nm flexion moment changes the risk by approximately 30%. Moreover, parametric morphing is based on the geometrical data and does not include any variation in the material properties. SAFER HBM v9 is currently not validated for predicting lumbar vertebra fractures, although a future version validated for predicting lumbar forces, moments, and vertebra fracture risk is under development.

The adaptive STLL effectively reduces the risk of lumbar vertebra fracture but it should be considered alongside alternative solutions. One other solution is to actively reposition the occupant in an upright position before the impact by means of electric drives in the seat. Such a solution, which would require accurate pre-crash sensing and relatively fast movement of the occupant, might be feasible in the future. However, before this solution is implemented, it must be determined that the fast movements themselves do not cause any harm to the occupant—and, further, that all possible crash scenarios are within the pre-crash sensors' operational design domain, so they can be detected and classified correctly.

In conclusion, an adaptive STLL, accommodating variations in HBM mass and frontal crash pulse severity, was shown to be beneficial, efficiently reducing the risk of lumbar and chest injuries for occupants seated in a relaxed position. However, more research is needed to reduce the injury risk in the high-severity crash pulse, enabled the activation strategy by developing an occupant monitoring system, and evaluated the strategy's robustness in other types of crashes (e.g., oblique frontal crashes).

## DATA AVAILABILITY STATEMENT

The datasets presented in this article are not readily available because the dataset belongs to Autoliv Development AB. The requests to access the datasets should be directed to martin.ostling@autoliv.com.

## AUTHOR CONTRIBUTIONS

MÖ and CL conceptualized the study and undertook the analysis. CL built and validated the simulation model, executed all simulations, and extracted all the results. MÖ planned and led the drafting of the manuscript in conjunction with NL and BP. All the authors were involved in interpreting the findings and drafting the manuscript.

## FUNDING

The work has received fundings from two sources: The work was partly carried out as part of the EU project SAFE-UP which has received funding from the European Union's Horizon 2020 research and innovation programme under Grant Agreement 861570. The work was partly carried out in the project 2020-

## REFERENCES

- Adomeit, D. (1977). Evaluation Methods for the Biomechanical Quality of Restraint Systems during Frontal Impact. *SAE Technical Paper 770936*. doi:10.4271/770936
- Adomeit, D., and Heger, A. (1975). Motion Sequence Criteria and Design Proposals for Restraint Devices in Order to Avoid Unfavourable Biomechanics Conditions and Submarining. *SAE Technical Paper 751146*. doi:10.4271/751146
- Association for the Advancement of Automotive Medicine (AAAM) (2015). *The Abbreviated Injury Scale*. Chicago, IL: Association for the Advancement of Automotive Medicine 35 E Wacker Drive Ste
- Bilston, L. E., Clarke, E. C., and Brown, J. (2011). Spinal Injury in Car Crashes: Crash Factors and the Effects of Occupant Age. *Inj. Prev.* 17 (4), 228–232. doi:10.1136/ip.2010.028324
- Bohlin, N., Hallen, A., Runberger, S., and AASberg, A. (1978). Safety and Comfort - Factors in Volvo Occupant Compartment Packaging. *SAE Tech.* doi:10.4271/780135
- Boyle, K. J., Reed, M. P., Zaseck, L. W., and Hu, J. (2019). "A Human Modelling Study on Occupant Kinematics in Highly Reclined Seats during Frontal Crashes," in Proceedings of IRCOBI conference. Florence, Italy, September 11–13, 2019.
- Caballero-Bruno, I., Töpfer, D., Wohlbebe, T., and Hernández-Castellano, P. M. (2021). Novel Car Seat Posture Assessment through Comfort and User Experience. *Proceeding Conf. Congr.* 2021.
- Craig, M., Parent, D., Lee, E., Rudd, R., Takhounts, E., and Hasija, V. (2020). *Injury Criteria for the THOR 50th Male ATD*. Available at: <https://lindseyresearch.com/wp-content/uploads/2021/10/NHTSA-2020-0032-0005-Injury-Criteria-for-the-THOR-50th-Male-ATD.pdf> (Accessed February 17, 2022).
- Dissanaike, S., Kaufman, R., Mack, C. D., Mock, C., and Bulger, E. (2008). The Effect of Reclined Seats on Mortality in Motor Vehicle Collisions. *J. Trauma Inj. Infect. Crit. Care March* 64, 614–619. doi:10.1097/TA.0b013e318164d071
- Dobberstein, J., Schmidt, D., Östling, M., Bálint, A., Lindman, M., and Höschele, P. (2021). Final Results on Detailed Crash Configurations from Collisions Expected to Remain for Automated Vehicles. *OSCCAR Proj. Deliv.* 3, 2021. Available at: <https://www.osccarproject.eu/>.

02943 Car Passenger Safety–To the Next Level, which has received funding from FFI (Strategic Vehicle Research and Innovation), Vinnova (Sweden's Innovation Agency), the Swedish Transport Administration, the Swedish Energy Agency, and the Swedish vehicle industry.

## ACKNOWLEDGMENTS

The authors would like to thank Karl-Johan Larsson at Autoliv Research for executing the parametrized morphing of the SAFER HBM v9 to the anthropometry of a large 65-year-old male and for providing fundamentally important feedback and discussions on how to use and extract results from the SAFER HBM. Furthermore, the authors would like to thank Kristina Mayberry for language revisions.

## SUPPLEMENTARY MATERIAL

The Supplementary Material for this article can be found online at: <https://www.frontiersin.org/articles/10.3389/ffutr.2022.890117/full#supplementary-material>

- Forman, J. L., Kent, R. W., Mroz, K., Pipkorn, B., Bostrom, O., and Segui-Gomez, M. (2012). Predicting Rib Fracture Risk with Whole-Body Finite Element Models: Development and Preliminary Evaluation of a Probabilistic Analytical Framework. *Ann. Adv. Automot. Med.* 56, 109–124.
- Forman, J. L., and McMurry, T. L. (2018). Nonlinear Models of Injury Risk and Implications in Intervention Targeting for Thoracic Injury Mitigation. *Traffic Inj. Prev.* 19, S103–S108. doi:10.1080/15389588.2018.1528356
- Fryar, C. D., Gu, Q., Ogden, C. L., and Flegal, K. M. (2016). Anthropometric Reference Data for Children and Adults: United States, 2011–2014. *National Center for Health Statistics. Vital Health Stat.* 3 (39), 9–15.
- Höschele, P., Smit, S., Tomasch, E., Östling, M., Mroz, K., and Klug, C. (2021). *Generic Crash Pulses Representative for Future Accident Scenarios of Highly Automated Vehicles*, *SAE International Journal of Transportation Safety, Special Issue on Occupant Protection & Crashworthiness for ADS-Equipped Vehicles*. doi:10.3217/datacite.2400t-cxv49
- Hwang, E., Hu, J., Chen, C., Klein, K. F., Miller, C. S., Reed, M. P., et al. (2016). Development, Evaluation, and Sensitivity Analysis of Parametric Finite Element Whole-Body Human Models in Side Impacts. *Stapp Car Crash J.* 60 (November), 473–508. doi:10.4271/2016-22-0014
- Iraeus, J., and Pipkorn, B. (2019). "Development and Validation of a Generic Finite Element Ribcage to Be Used for Strain Based Fracture Prediction," in Proceedings of the IRCOBI Conference, Florence, Italy, September 11–13, 2019.
- Iraeus, J. (20152015). "Stochastic Finite Element Simulations of Real Life Frontal Crashes: With Emphasis on Chest Injury Mechanisms in Near-Side Oblique Loading Conditions," (Sweden: Faculty of Medicine, Department of Surgical and Perioperative Sciences, Surgery, Umeå University). PhD Thesis.
- Iwamoto, M., Kisanuki, Y., Watanabe, I., Furusu, K., Miki, K., and Hasegawa, J. (2002). "Development of a Finite Element Model of the Total Human Model for Safety (THUMS) and Application to Injury Reconstruction," in Proceedings of IRCOBI Conference, Munich, Germany, 2002-9-18 to 2002-9-20.
- Jakobsson, L., Bergman, T., and Johansson, L. (2006). "Identifying Thoracic and Lumbar Spinal Injuries in Car Accidents," In Proceedings of IRCOBI Conference on Biomechanics of Impacts, Madrid, September 20–22, 2006.
- Ji, P., Huang, Y., and Zhou, Q. (2017). Mechanisms of Using Knee Bolster to Control Kinematical Motion of Occupant in Reclined Posture for Lowering Injury Risk. *Int. J. Crashworthiness* 22 (4), 415–424. doi:10.1080/13588265.2016.1275430

- Koppel, S., Jiménez Octavio, J., Bohman, K., Logan, D., Raphael, W., Quintana Jimenez, L., et al. (2019). Seating Configuration and Position Preferences in Fully Automated Vehicles. *Traffic Inj. Prev.* 20, S103–S110. doi:10.1080/15389588.2019.1625336
- Larsson, K.-J., Pipkorn, B., Iraeus, J., Forman, J., and Hu, J. (2021). Evaluation of a Diverse Population of Morphed Human Body Models for Prediction of Vehicle Occupant Crash Kinematics. *Comput. Methods Biomechanics Biomed. Eng.*, 1–31. doi:10.1080/10255842.2021.2003790
- Luo, M., and Zhou, Q. (2010). A Vehicle Seat Design Concept for Reducing Whiplash Injury Risk in Low-Speed Rear Impact. *Int. J. Crashworthiness* 15 (3), 293–311. doi:10.1080/13588260903335282
- McMurry, T. L., Poplin, G. S., Shaw, G., and Panzer, M. B. (2018). Crash Safety Concerns for Out-Of-Position Occupant Postures: A Look toward Safety in Highly Automated Vehicles. *Traffic Inj. Prev.* 19 (6), 582–587. doi:10.1080/15389588.2018.1458306
- Mertz, H., Irwin, A., Melvin, J., Stalnaker, R., and Beebe, M. (1989). *Size, Weight and Biomechanical Impact Response Requirements for Adult Size Small Female and Large Male Dummies*. Detroit, MI: SAE International Congress and Exposition.
- Moreau, D., Donlon, J. P., Richardson, R., and Gepner, B. (2021). “A Methodology to Replicate Lap Belt Loading Conditions from a Sled Impact Test in a Non-impact Dynamic Environment on Whole-Body Postmortem Human Subjects,” in Proceedings of IRCOBI Conference, September 8–10, 2021.
- Mroz, K., Östling, M., Klug, C., Höschele, P., and Lubbe, N. (2022). Supplementing Future Occupant Safety Assessments with Critical Intersection Crashes Selected Using the SAFER Human Body Model. *SAE Int. J. Trans. Saf.* 2021.
- Mroz, K., Östling, M., Richardson, R., Kerrigan, J., Forman, J., Gepner, B., et al. (2020). “Effect of Seat and Seat Belt Characteristics on the Lumbar Spine and Pelvis Loading of the SAFER Human Body Model in Reclined Postures,” in Proceedings of the IRCOBI Conference, Munich, Germany.
- Ortiz-Paparoni, M., Op ’t Eynde, J., Kait, J., Bigler, B., Shridharani, J., Schmidt, A., et al. (2021). The Human Lumbar Spine during High-Rate under Seat Loading: A Combined Metric Injury Criteria. *Ann. Biomed. Eng.* 49 (11), 3018–3030. doi:10.1007/s10439-021-02823-x
- Östling, J., Bohman, K., and Jakobsson, L. (2020). “Evaluation of Kinematics and Restraint Interaction when Repositioning a Driver from a Reclined to Upright Position Prior to Frontal Impact Using Active Human Body Model Simulations,” in Proceedings of the IRCOBI Conference, Munich, Germany.
- Östling, M., and Larsson, A. (2019). “Occupant Activities and Sitting Positions in Automated Vehicles in China and Sweden,” in Proceedings of Conference for the Enhancement of Safety Vehicles (ESV), 2019, Eindhoven, Netherlands, June 10–13, 2019.
- Östling, M., Lundgren, C., Lubbe, N., Huf, A., Wernicke, P., and Pipkorn, B. (2021). “The Influence of a Seat Track Load Limiter on Lumbar Spine Compression Forces in Relaxed, Reclined, and Upright Seating Positions: A Sled Test Study Using THOR-50M,” in Proceedings of the IRCOBI Conference, September 8–10, 2021.
- Östling, M., Sunnevång, C., Svensson, C., and Kock, H. O. (2017). *Potential Future Seating Positions and the Impact on Injury Risks in a Learning Intelligent Vehicle (LIV)*. Berlin, Germany: VDI-Tagung Fahrzeugsicherheit.
- Pipkorn, B., Iraeus, J., Björklund, M., Bunketorp, O., and Jakobsson, L. (2019). “Multi-Scale Validation of a Rib Fracture Prediction Method for Human Body Models,” in Proceedings of the IRCOBI Conference, 2019, Florence, Italy, September 11–13, 2019.
- Rao, R. D., Berry, C. A., Yoganandan, N., and Agarwal, A. (2014). Occupant and Crash Characteristics in Thoracic and Lumbar Spine Injuries Resulting from Motor Vehicle Collisions. *Spine J.* 14 (10), 2355–2365. doi:10.1016/j.spinee.2014.01.038
- Rawska, K., Gepner, B., and Kerrigan, J. R. (2021). Effect of Various Restraint Configurations on Submarining Occurrence across Varied Seat Configurations in Autonomous Driving System Environment. *Traffic Inj. Prev.* 22, S128–S133. doi:10.1080/15389588.2021.1939872
- Rawska, K., Gepner, B., Kulkarni, S., Chastain, K., Zhu, J., Richardson, R., et al. (2019). Submarining Sensitivity across Varied Anthropometry in an Autonomous Driving System Environment. *Traffic Inj. Prev.* 20, S123–S127. doi:10.1080/15389588.2019.1655734
- Reed, M. P., and Rupp, J. D. (2013). An Anthropometric Comparison of Current ATDs with the U.S. Adult Population. *Traffic Inj. Prev.* 14 (7), 703–705. doi:10.1080/15389588.2012.752819
- Richardson, R., Donlon, J. P., Jayathirtha, M., Forman, J. L., Shaw, G., Gepner, B., et al. (2020). Kinematic and Injury Response of Reclined PMHS in Frontal Impacts. *Stapp Car Crash J.* 64, 83–153. doi:10.4271/2020-22-0004
- Schneider, L. W., Robbins, D. H., Pflug, M. A., and Snyder, R. G. (1983). *Development of Anthropometrically Based Design Specifications for an Advanced Adult Anthropomorphic Dummy Family Report No: UMTRI-83-53-1*. Corporate Author: University of Michigan, Ann Arbor: Transportation Research Institute
- Sengottu Velavan, S., and Huf, A. (2018). “Development of Occupant Restraint Systems for Future Seating Positions in Fully or Semi Autonomous Vehicles,” in Proceedings of FISITA World Automotive Congress, 2018, Chennai, India, October 2–5, 2018.
- Stanglmeier, M. J., Paternoster, F. K., Paternoster, S., Bichler, R. J., Wagner, P. O., and Schwirtz, A. (2020). Automated Driving: A Biomechanical Approach for Sleeping Positions. *Appl. Ergon.* 86, 103103. doi:10.1016/j.apergo.2020.103103
- Stemper, B. D., Chirvi, S., Doan, N., Baisden, J. L., Maiman, D. J., Curry, W. H., et al. (2018). Biomechanical Tolerance of Whole Lumbar Spines in Straightened Posture Subjected to Axial Acceleration. *J. Orthop. Res.* 36 (6), 1747–1756. doi:10.1002/jor.23826
- Takata Corporation (2017). *Advanced Adaptive Restraint Systems. Report No. DOT HS 812 432*. Washington, DC: National Highway Traffic Safety Administration.
- Tang, L., Zheng, J., and Zhou, Q. (2020). Investigation of Risk Factors Affecting Injuries in Reclining Seat under Frontal Impact. *Int. J. Veh. Saf.* 11. doi:10.1504/ijvs.2020.109277
- Tushak, S. K., Gepner, B. D., Forman, J. L., Hallman, J. J., Pipkorn, B., and Kerrigan, J. R. (2022). *Human Lumbar Spine Injury Risk in High-Rate Combined Compression and Flexion Loading in Press* (Online ahead of print).
- Wiechel, J., and Bolte, J. (2006). *Response of Reclined Post Mortem Human Subjects to Frontal Impact*. SAE Technical Paper 2006-01-0674 2006. United State: SAE International. doi:10.4271/2006-01-0674
- Zhang, X., and Zhou, Q. (2016). An Energy-Absorbing Sliding Seat for Reducing Neck Injury Risks in Rear Impact-Analysis for Prototype Built. *Traffic Inj. Prev.* 17 (3), 313–319. doi:10.1080/15389588.2015.1064908

**Conflict of Interest:** The authors are employed at Autoliv in Vårgårda, Sweden. Autoliv ([www.autoliv.com](http://www.autoliv.com)) is a company that develops, manufactures, and sells protective safety systems to car manufacturers (among other products). Results from this study may impact how Autoliv choose to develop their products.

**Publisher’s Note:** All claims expressed in this article are solely those of the authors and do not necessarily represent those of their affiliated organizations, or those of the publisher, the editors, and the reviewers. Any product that may be evaluated in this article, or claim that may be made by its manufacturer, is not guaranteed or endorsed by the publisher.

Copyright © 2022 Östling, Lundgren, Lubbe and Pipkorn. This is an open-access article distributed under the terms of the Creative Commons Attribution License (CC BY). The use, distribution or reproduction in other forums is permitted, provided the original author(s) and the copyright owner(s) are credited and that the original publication in this journal is cited, in accordance with accepted academic practice. No use, distribution or reproduction is permitted which does not comply with these terms.